arXiv:1211.4743v1 [hep-ph] 20 Nov 2012

Revisiting the gravitino dark matter and baryon asymmetry from Q-ball decay in gauge mediation

Shinta Kasuya^{a,b}, Masahiro Kawasaki^{c,d} and Masaki Yamada^{c}
^{a} *Department of Mathematics and Physics, Kanagawa University, Kanagawa 259-1293, Japan*
^{b} *Max-Planck-Institut für Kernphysik, PO Box 103980, 69029 Heidelberg, Germany*
^{c} *Institute for Cosmic Ray Research, University of Tokyo, Chiba 277-8582, Japan*
^{d} *Kavli Institute for the Physics and Mathematics of the Universe, University of Tokyo, Chiba 277-8582, Japan*

(Dated: November 20, 2012)

We reinvestigate the scenario that the amount of the baryons and the gravitino dark matter is naturally explained by the decay of the Q balls in the gauge-mediated SUSY breaking. Equipped by the more correct decay rates into gravitinos and baryons recently derived, we find that the scenario with the direct production of the gravitino dark matter from the Q-ball decay works naturally.

I. INTRODUCTION

The abundances of the baryons and dark matter are almost comparable in the present universe. It may be understood by the fact that both of them have the same origin: Q balls. The Q balls are nontopological solitons whose stability is guaranteed by the finite charge Q [1]. In supersymmetry (SUSY), they are produced during the course of the Affleck-Dine baryogenesis [2–6], so the charge Q is essentially the baryon number.

In the gauge-mediated SUSY breaking, very large Q balls are stable against the decay into nucleons, the lightest particle with a unit baryon number. On the other hand, if the charge Q is small enough, the Q balls could decay into nucleons (baryons). In the latter case, the gravitinos are also produced by the Q-ball decay. The gravitino is the lightest SUSY particle in the gauge mediation. Therefore, there may be the way to provide both the baryons and the dark matter in the universe by the Q-ball decay [7–10].

In Ref. [9], two of the present authors investigated the scenario to explain both the baryon asymmetry and the dark matter in the universe by the Q-ball decay, considering the decays into nucleons (quarks), gravitinos, and the next to lightest SUSY particles (NLSPs), taking into account the big bang nucleosynthesis (BBN) limits of NLSP abundances. Recently in Ref. [11], however, another two of us studied the Q-ball decay more correctly, and found that the decay rate into gravitinos is much smaller than that estimated in Ref. [9]. The essence is to consider the finite size of the Q ball which becomes smaller than the penetration length of the decay particle in the actual gauge-mediation Q ball. Therefore, it is necessary to reanalyze whether this attractive scenario works or not, and this is the purpose of the present article.

As we will see, it is natural to achieve the right amounts of the baryon asymmetry and the gravitino dark matter at the same time through the direct production from the Q-ball decay although we find the branching into gravitinos becomes smaller than the previous estimate in Ref.[9]. In this case, more NLSPs are produced by the Q-ball decay, but they annihilate afterwards [10] and the remaining NLSP provides only the negligible amount of the gravitinos to the dark matter density. Moreover, even for $m_{3/2} \gtrsim$ GeV, severe BBN constraints could be avoided if the Q-ball decay temperature is high enough.

The structure of the article is as follows. In the next section, we review the basic features of the Q ball in the gauge-mediated SUSY breaking. In Sec.III, we provide the decay rates of the Q ball, extracted from Ref. [11]. In Sec.IV, we reestimate the abundances of the baryons, the gravitinos, and the NLSPs, and seek for the working parameters in Sec.V. We conclude in Sec.VI. In the appendix, we show, for completeness, some results concerned with so-called indirect case where the gravitino dark matter is produced by the decay of the NLSPs which are created by the Q-ball decay.

II. Q BALL IN THE GAUGE MEDIATION

The Q ball is constructed from the scalar field called the flat direction in SUSY theories. It consists of squarks and sleptons, and the potential is given by [12]

$$V(\Phi) = \begin{cases} m_\phi^2 |\Phi|^2, & (|\Phi| \ll M_S), \\ M_F^4 \left(\log \frac{|\Phi|^2}{M_S^2}\right)^2, & (|\Phi| \gg M_S), \end{cases} \tag{1}$$

in the gauge-mediated SUSY breaking[1]. Here $m_\phi \sim O(\mathrm{TeV})$ is a soft breaking mass, and M_F and M_S are related to the F and A components of a gauge-singlet chiral multiplet S in the messenger, respectively, as

$$M_F^4 \equiv \frac{g^2}{(4\pi)^4} \langle F_A \rangle^2, \qquad M_S \equiv \langle S \rangle, \tag{2}$$

where g stands for the gauge coupling in the standard model in general. M_F ranges as

$$10^3 \text{ GeV} \lesssim M_F \lesssim \frac{g^{1/2}}{4\pi} \sqrt{m_{3/2} M_{\mathrm{P}}}, \tag{3}$$

---

[1] M_F and m_ϕ are related to parameters used in Ref. [11] as $M_F = 2^{-1/4}(m_s M_m/g)^{1/2}$ and $m_\phi = \sqrt{2} m_s$, respectively.

where $m_{3/2}$ is the gravitino mass, and $M_{\rm P}(\approx 2.4\times10^{18}$ GeV) is the reduced Planck scale.

Q balls form from the condensate of the flat direction during its helical motion after it started rotation when $H\sim M_F^2/\phi_{\rm osc}$, where $\phi_{\rm osc}$ is the amplitude at the onset of rotation. The charge of the created Q ball is estimated as [6]

$$Q=\beta\left(\frac{\phi_{\rm osc}}{M_F}\right)^4, \tag{4}$$

where $\beta\simeq6\times10^{-4}$ for a circular orbit ($\varepsilon=1$), while $\beta\simeq6\times10^{-5}$ for an oblate case ($\varepsilon\lesssim0.1$). Here ε denotes the ellipticity of the field orbit. The charge Q is in fact the Φ-number, and relates to the baryon number of the Q ball as

$$B=bQ. \tag{5}$$

Here we assign the baryon number b to Φ-particle. For example, $b=1/3$ for the *udd* direction. The mass, the size, the rotation speed of the field, and the field amplitude at the center of the Q ball are expressed in terms of the charge Q respectively as

$$M_Q\simeq\frac{4\sqrt{2}\pi}{3}\zeta M_F Q^{3/4}, \tag{6}$$

$$R_Q\simeq\frac{1}{\sqrt{2}}\zeta^{-1}M_F^{-1}Q^{1/4}, \tag{7}$$

$$\omega_Q\simeq\sqrt{2}\pi\zeta M_F Q^{-1/4}, \tag{8}$$

$$\phi_Q\simeq\frac{1}{\sqrt{2}}\zeta M_F Q^{1/4}, \tag{9}$$

where ζ is $O(1)$ parameter determined by the fit to numerical calculation [11, 13][2].

The Q ball can decay into those particles kinematically allowed. This condition is written as $\omega_Q>m_{\rm decay}$. Since we are interested in the production of baryons, it is rephrased as $\omega_Q>bm_N$, where $m_N\simeq1$ GeV is the nucleon mass, or $\omega_Q>m_q$ before the confinement, where m_q is the quark mass. In this article, we adopt the bottom mass so that $m_q=m_b\approx4.2$ GeV [3], although it depends on when the Q balls decay and which flat direction it is, for example. This leads to $Q<Q_{\rm D}$ with

$$Q_{\rm D}=4\pi^4\zeta^4\left(\frac{M_F}{m_b}\right)^4. \tag{10}$$

Similarly, the Q ball decays into NLSPs, once the condition $\omega_Q>m_{\rm NLSP}$ is met. This leads to the charge smaller than $Q_{\rm cr}$, where

$$Q_{\rm cr}=4\pi^4\zeta^4\left(\frac{M_F}{m_{\rm NLSP}}\right)^4. \tag{11}$$

III. Q-BALL DECAY

The decay rate of the Q ball has an upper bound as [11][4].

$$\Gamma_Q\lesssim\Gamma_Q^{\rm (sat,d)}\simeq\frac{1}{Q}\frac{\omega_Q^3}{96\pi^2}4\pi R_Q^2, \tag{12}$$

derived by considering the maximum outgoing flow of the fermions χ, which has coupling $\mathcal{L}_{\rm int}=f\phi^*\chi\eta+$h.c., in the limite of $R_Q\omega_Q\to\infty$, and is valid typically for $f\phi_Q\gtrsim\omega_Q$. Here we put the index d, since the elementary process is the decay $\phi\to\chi+\eta$. This rate is applicable to the Q-ball decay into NLSPs, and it actually expresses as $\Gamma_Q^{\rm (NLSP)}\simeq1.4\,\Gamma_Q^{\rm (sat,d)}$ [11].

On the other hand, the elementary process of the Q-ball decay into quarks when $\omega_Q<m_{\rm NLSP}$ takes place through heavy gluino (or higgsino) exchange as $\phi+\phi\to q+q$. Since quarks can possess twice larger momenta than in the decay case, ω_Q in the decay rate should be replaced by $2\omega_Q$, so that, for the scattering, we have [11]

$$\Gamma_Q^{\rm (sat,s)}\simeq\frac{1}{Q}\frac{\omega_Q^3}{12\pi^2}4\pi R_Q^2. \tag{13}$$

Numerical calculation in Ref. [11] provides the prefactor, and the decay rate into quarks is given by

$$\Gamma_Q^{\rm (q)}\simeq1.1\,N_q\Gamma_Q^{\rm (sat,s)}, \tag{14}$$

where N_q is the possible degrees of freedom of quarks, and we set it as $3\times3\times2=18$ in the following. This is indeed the Q-ball decay rate that is used for the decay into baryons.

In the opposite case of $f\phi_Q\ll\omega_Q$, the rate was estimated in Ref. [14] as

$$\Gamma_Q\simeq3\pi\frac{f\phi_Q}{\omega_Q}\Gamma_Q^{\rm (sat)}, \tag{15}$$

for $R_Q\omega_Q\to\infty$, whose physical meaning can be understood as follows [11]. The interaction region is only the surface layer of the Q ball whose depth is given by the penetration length of produced particles $\sim(f\phi_Q)^{-1}$. Therefore the decay rate can be estimated as the product of one-particle decay rate ($\sim f^2\omega_Q$), particle density ($\sim\omega_Q\phi_Q^2$), and the effective volume ($\sim4\pi R_Q^2(f\phi_Q)^{-1}$).

---

[2] The actual value is estimated as $\zeta=2^{1/4}\sqrt{c/\pi}$, where $c=4.8\log(m_s/\omega_0)+7.4$ in terms of parameters used in Ref. [11]. In our successful scenario, typically $c\approx14$, so that $\zeta\approx2.5$.

[3] Results do not change even if we take the top quark mass, since this condition is less restrictive. See Sec. V.

[4] The decay rate was first derived in Ref.[14]. It is different from the present result by factor 2, since they show the pair production rate in the theory of $\chi=\eta$.

However, it was pointed out in Ref. [11, 13] that this is not the case for realistic Q balls in SUSY. In fact, the size of the Q ball is $R_Q \sim \omega_Q^{-1}$, so that the penetration length of the produced particles becomes larger than the Q-ball size: $(f\phi_Q)^{-1} \gg \omega_Q^{-1} \sim R_Q$. Therefore, the effective volume should be the whole volume of the Q ball. Then the decay rate has the following dependence:

$$\Gamma_Q \sim \left(\frac{f\phi_Q}{\omega_Q}\right)^2 \Gamma_Q^{(\mathrm{sat,d})}. \tag{16}$$

The Q-ball decay into gravitinos is then given by [11]

$$\Gamma_Q^{(3/2)} \simeq 0.9 \left(\frac{\omega_Q \phi_Q}{\langle F\rangle}\right)^2 \Gamma_Q^{(\mathrm{sat,d})}, \tag{17}$$

where $\langle F\rangle = \sqrt{3} m_{3/2} M_\mathrm{P}$ is the SUSY breaking F term.

IV. ABUNDANCES

Now we have in our hand the revised decay rates into baryons (14) and into gravitinos (17). Since the main decay channel is the decay into baryons, the temperature at the decay is given by

$$\begin{aligned} T_\mathrm{D} &= \left(\frac{90}{4\pi^2 N_\mathrm{D}}\right)^{1/4} \sqrt{\Gamma_Q^{(\mathrm{q})} M_\mathrm{P}}, \\ &\simeq 0.58 \text{ GeV} \left(\frac{\zeta}{2.5}\right)^{1/2} \left(\frac{N_q}{18}\right)^{1/2} \left(\frac{N_\mathrm{D}}{61.75}\right)^{-1/4} \\ &\quad \times \left(\frac{M_F}{10^7 \text{ GeV}}\right)^{1/2} \left(\frac{Q}{10^{22}}\right)^{-5/8}, \end{aligned} \tag{18}$$

where N_D is the relativistic degrees of freedom at the decay time.

Refining the estimates of the baryon and gravitino abundances together with NLSP abundance, which are produced by the Q-ball decay, we have the relations between those number densities and that of the ϕ field as [9]

$$n_b \simeq \varepsilon b n_\phi, \tag{19}$$

$$n_{3/2} \simeq B_{3/2} n_\phi, \tag{20}$$

$$n_\mathrm{NLSP} \simeq B_\mathrm{NLSP} \frac{Q_\mathrm{cr}}{Q} n_\phi, \tag{21}$$

where $B_{3/2} \simeq \Gamma_Q^{(3/2)}/\Gamma_Q^{(\mathrm{q})}$ is the branching ratio of the decay into gravitinos estimated as

$$\begin{aligned} B_{3/2} &\simeq 1.3 \times 10^{-7} \left(\frac{\zeta}{2.5}\right)^4 \left(\frac{N_q}{18}\right)^{-1} \\ &\quad \times \left(\frac{M_F}{10^7 \text{ GeV}}\right)^4 \left(\frac{m_{3/2}}{100 \text{ MeV}}\right)^{-2}. \end{aligned} \tag{22}$$

On the other hand, the branching into NLSPs is derived as

$$B_\mathrm{NLSP} \simeq \frac{\Gamma_Q^{(\mathrm{NLSP})}}{\Gamma_Q^{(\mathrm{q})}} \simeq 8.8 \times 10^{-3} \left(\frac{N_q}{18}\right)^{-1}, \tag{23}$$

once it is allowed kinematically when $Q < Q_\mathrm{cr}$. If the charge Q is smaller than Q_cr when the Q ball formed, one should set $Q_\mathrm{cr}/Q = 1$ in Eq.(21).

The actual abundances are dependent on whether or not Q balls dominate the energy density of the universe before the decay. The baryon abundances for the Q-ball dominated (QD) and non-Q-ball dominated (NQD) cases are thus given by

$$Y_b \equiv \frac{n_b}{s} = \begin{cases} \dfrac{3T_\mathrm{D}}{4} \dfrac{n_b}{\rho_Q}\Big|_\mathrm{D} = \dfrac{3T_\mathrm{D}}{4} \dfrac{n_b}{\rho_Q}\Big|_\mathrm{osc} & \\ \qquad \simeq \dfrac{3T_\mathrm{D}}{4} \dfrac{\varepsilon b n_\phi}{\frac{4}{3}\omega_Q n_\phi} \simeq \dfrac{9T_\mathrm{D}\varepsilon b}{16\omega_Q}, & \text{(QD)} \\ \dfrac{3T_\mathrm{RH}}{4} \dfrac{n_b}{\rho_\mathrm{rad}}\Big|_\mathrm{RH} = \dfrac{3T_\mathrm{RH}}{4} \dfrac{n_b}{\rho_\mathrm{inf}}\Big|_\mathrm{osc} & \\ \qquad \simeq \dfrac{9}{8\sqrt{2}} \varepsilon b \beta^{-3/4} \dfrac{M_F T_\mathrm{RH}}{M_\mathrm{P}^2} Q^{3/4}, & \text{(NQD)} \end{cases} \tag{24}$$

where Eq.(19) and

$$\rho_Q \simeq M_Q n_Q \simeq M_Q \frac{n_\phi}{Q} \simeq \frac{4}{3}\omega_Q n_\phi, \tag{25}$$

are used in the QD case, while $n_\phi \simeq m_\mathrm{eff}\phi_\mathrm{osc}^2$, $m_\mathrm{eff} = \sqrt{V''} \simeq 2\sqrt{2} M_F^2/\phi_\mathrm{osc}$, $3H_\mathrm{osc} = m_\mathrm{eff}$, and Eq.(4) are used in the NQD case. On the other hand, the abundance of the gravitino dark matter is determined by the ratio with the baryon density as

$$5 \approx \frac{\rho_{3/2}}{\rho_b} = \frac{m_{3/2}}{m_N} \frac{n_{3/2}}{n_b} \simeq \frac{m_{3/2}}{m_N} \frac{B_{3/2}}{\varepsilon b}. \tag{26}$$

Therefore, we can eliminate εb in Eq.(24) using Eq.(26) to obtain the baryon abundance as, setting $\beta = 6 \times 10^{-5}$,

$$\begin{aligned} \frac{Y_b^{(\mathrm{QD})}}{10^{-10}} &\simeq 2.4 \times 10^{-2} \left(\frac{\zeta}{2.5}\right)^{7/2} \left(\frac{N_q}{18}\right)^{-1/2} \left(\frac{N_\mathrm{D}}{61.75}\right)^{-1/4} \\ &\quad \times \left(\frac{m_{3/2}}{100 \text{ MeV}}\right)^{-1} \left(\frac{M_F}{10^7 \text{ GeV}}\right)^{7/2} \left(\frac{Q}{10^{22}}\right)^{-3/8}, \end{aligned} \tag{27}$$

and

$$\begin{aligned} \frac{Y_b^{(\mathrm{NQD})}}{10^{-10}} &\simeq 1.6 \times 10^{-5} \left(\frac{\zeta}{2.5}\right)^4 \left(\frac{N_q}{18}\right)^{-1} \\ &\quad \times \left(\frac{m_{3/2}}{100 \text{ MeV}}\right)^{-1} \left(\frac{T_\mathrm{RH}}{10^4 \text{ GeV}}\right) \\ &\quad \times \left(\frac{M_F}{10^7 \text{ GeV}}\right)^5 \left(\frac{Q}{10^{22}}\right)^{3/4}, \end{aligned} \tag{28}$$

for the Q-ball dominance and non-dominance, respectively. These relations must be hold for simultaneous explanation of the baryon and gravitino dark matter abundances.

The NLSP abundance produced by the Q-ball decay is estimated as

$$\begin{aligned}\frac{\rho^{(Q)}_{\rm NLSP}}{s} &= m_{3/2}Y_{3/2}\frac{\rho_{\rm NLSP}}{\rho_{3/2}} \simeq 5m_N Y_b \frac{m_{\rm NLSP}}{m_{3/2}}\frac{n_{\rm NLSP}}{n_{3/2}} \\ &\simeq 5m_N Y_b \frac{m_{\rm NLSP}}{m_{3/2}}\frac{B_{\rm NLSP}Q_{\rm cr}}{B_{3/2}Q} \\ &\simeq 0.20\ {\rm GeV}\left(\frac{Y_b}{10^{-10}}\right)\left(\frac{m_{3/2}}{100\ {\rm MeV}}\right) \\ &\qquad \times\left(\frac{m_{\rm NLSP}}{300\ {\rm GeV}}\right)^{-3}\left(\frac{Q}{10^{22}}\right)^{-1}, \qquad (29)\end{aligned}$$

at the decay time. Here and hereafter we take $m_{\rm NLSP} = 300$ GeV, although we keep showing its dependence. It is shown for some fixed value of the charge Q in the dark green dotted-dashed lines in Fig. 1.

The NLSP abundance is usually determined by the subsequent annihilations of NLSPs as $n^{(\rm ann)}_{\rm NLSP} \simeq H(T_{\rm D})/\langle\sigma v\rangle$ [10]. The annihilation cross sections for the bino, stau, and sneutrino NLSP are estimated as [15]

$$\langle\sigma v\rangle_{\tilde B} \simeq 1.5\times 10^{-10}{\rm GeV}^{-2}\left(\frac{m_{\rm NLSP}}{300\ {\rm GeV}}\right)^{-2}, \qquad (30)$$

$$\langle\sigma v\rangle_{\tilde\tau} \simeq 7.4\times 10^{-9}{\rm GeV}^{-2}\left(\frac{m_{\rm NLSP}}{300\ {\rm GeV}}\right)^{-2}, \qquad (31)$$

$$\langle\sigma v\rangle_{\tilde\nu} \simeq 2.5\times 10^{-8}{\rm GeV}^{-2}\left(\frac{m_{\rm NLSP}}{300\ {\rm GeV}}\right)^{-2}. \qquad (32)$$

They lead to

$$\begin{aligned}\left.\frac{\rho^{(\rm ann)}_{\rm NLSP}}{s}\right|_{\tilde B} &\simeq 2.0\times 10^{-4}\ {\rm GeV}\left(\frac{N_{\rm D}}{10.75}\right)^{-1/2} \\ &\qquad\times\left(\frac{m_{\rm NLSP}}{300\ {\rm GeV}}\right)^{3}\left(\frac{T_{\rm D}}{\rm MeV}\right)^{-1}, \qquad (33)\\ \left.\frac{\rho^{(\rm ann)}_{\rm NLSP}}{s}\right|_{\tilde\tau} &\simeq 3.9\times 10^{-6}\ {\rm GeV}\left(\frac{N_{\rm D}}{10.75}\right)^{-1/2} \\ &\qquad\times\left(\frac{m_{\rm NLSP}}{300\ {\rm GeV}}\right)^{3}\left(\frac{T_{\rm D}}{\rm MeV}\right)^{-1}, \qquad (34)\\ \left.\frac{\rho^{(\rm ann)}_{\rm NLSP}}{s}\right|_{\tilde\nu} &\simeq 1.2\times 10^{-6}\ {\rm GeV}\left(\frac{N_{\rm D}}{10.75}\right)^{-1/2} \\ &\qquad\times\left(\frac{m_{\rm NLSP}}{300\ {\rm GeV}}\right)^{3}\left(\frac{T_{\rm D}}{\rm MeV}\right)^{-1}. \qquad (35)\end{aligned}$$

When the density of the NLSP produced from Q-ball decay is larger than the annihilation density, $\rho^{(Q)}_{\rm NLSP} > \rho^{(\rm ann)}_{\rm NLSP}$, the NLSP density will settle down to the annihilation value in the end. The annihilation abundances are displayed for several different decay temperatures $T_{\rm D}$ in blue solid lines in Fig. 1.

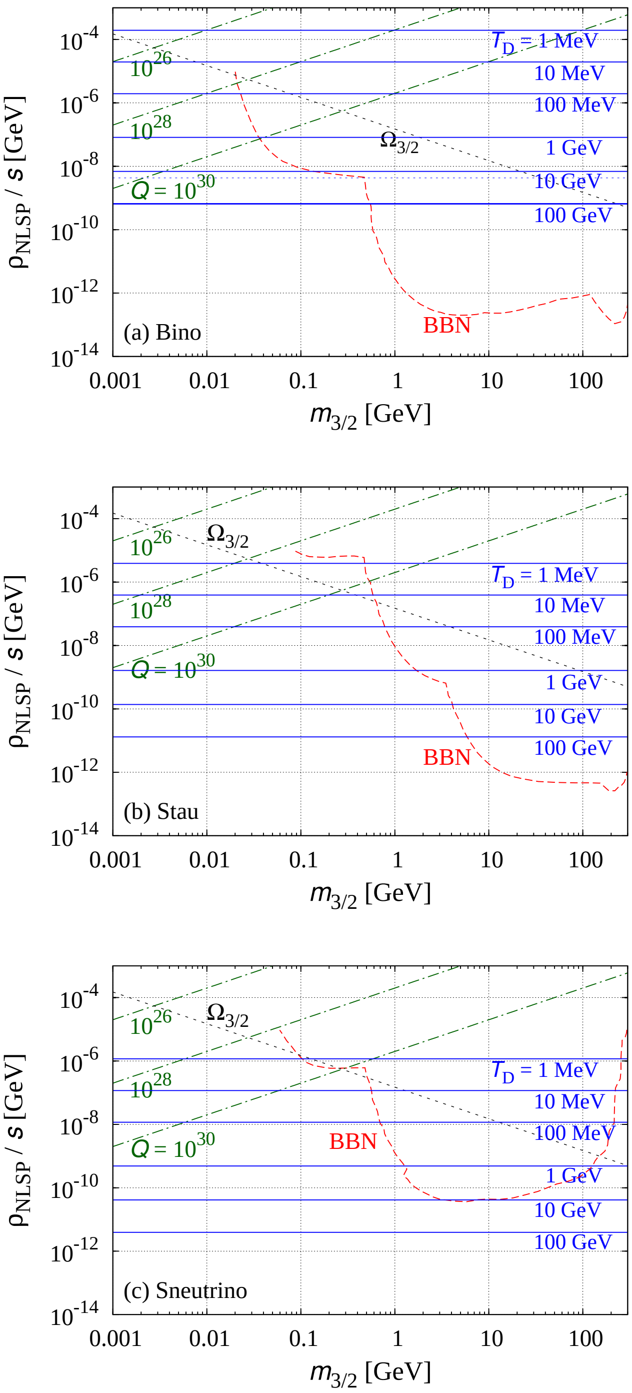

FIG. 1: NLSP abundances produced by the Q-ball decay for $Q = 10^{26}$, 10^{28}, and 10^{30} in dark green dotted-dashed lines. The abundances fixed by the annihilation is denoted by blue solid lines. Black dotted line is the abundance that the NLSP decay gives the right amount of the gravitino dark matter. Red dashed lines are the BBN constraints [16].

The abundance is generally limited by the BBN bound for each species of NLSP [16], shown in red dashed lines, or bounded by the NLSP abundance that accounts the right amount of the gravitino dark matter by the NLSP decay, denoted by black dotted line. The latter limit is given by [9, 16]

$$\left.\frac{\rho_{\rm NLSP}}{s}\right|_{\Omega_{3/2}} = 1.5\times10^{-6}\ {\rm GeV}\left(\frac{m_{\rm NLSP}}{300\ {\rm GeV}}\right) \times\left(\frac{m_{3/2}}{100\ {\rm MeV}}\right)^{-1}\left(\frac{Y_b}{10^{-10}}\right). \quad (36)$$

As we see later, the Q-ball charge is $\lesssim 10^{26}$, so that the NLSP abundance is fixed by the annihilation density. Therefore, for larger decay temperature $T_{\rm D}$, which will be achieved in the successful scenario, the gravitinos produced by the decay of NLSPs can entirely be negligible for the gravitino dark matter abundance. Moreover, severe BBN constraints are evaded, and we can take larger gravitino mass $m_{3/2}$ for successful scenarios.

V. CONSTRAINING MODEL PARAMETERS

Our scenario simultaneously explains the right amount of the baryon asymmetry and the gravitino dark matter both from the Q-ball decay. Since $Y_b \simeq 10^{-10}$, for successful scenario, we can obtain, from Eqs.(27) and (28), the relations that hold for the charge Q as

$$Q \simeq 4.7\times10^{17}\left(\frac{\zeta}{2.5}\right)^{28/3}\left(\frac{N_q}{18}\right)^{-4/3}\left(\frac{N_{\rm D}}{61.75}\right)^{-2/3} \times\left(\frac{m_{3/2}}{100\ {\rm MeV}}\right)^{-8/3}\left(\frac{M_F}{10^7\ {\rm GeV}}\right)^{28/3}, \quad (37)$$

$$Q \simeq 2.4\times10^{28}\left(\frac{\zeta}{2.5}\right)^{-16/3}\left(\frac{N_q}{18}\right)^{4/3}\left(\frac{m_{3/2}}{100\ {\rm MeV}}\right)^{4/3} \times\left(\frac{T_{\rm RH}}{10^4\ {\rm GeV}}\right)^{-4/3}\left(\frac{M_F}{10^7\ {\rm GeV}}\right)^{-20/3}, \quad (38)$$

for QD and NQD cases, respectively. The latter is dependent on the reheating temperature after inflation, $T_{\rm RH}$. It has un upper bound so that thermally produced gravitinos do not overdominate the universe, which results in [17]

$$T_{\rm RH} \lesssim 3\times10^6\ {\rm GeV}\left(\frac{m_{3/2}}{100\ {\rm MeV}}\right). \quad (39)$$

Taking account of this upper bound in Eq.(38), we obtain the lower limit as

$$Q \simeq 1.2\times10^{25}\left(\frac{\zeta}{2.5}\right)^{-16/3}\left(\frac{N_q}{18}\right)^{4/3}\left(\frac{M_F}{10^7\ {\rm GeV}}\right)^{-20/3}. \quad (40)$$

Notice that it is independent of $m_{3/2}$. Eqs.(37) and (40) are shown in blue solid and red dashed lines, respectively, in Fig. 2.

(a) $m_{3/2}$ = 100 MeV

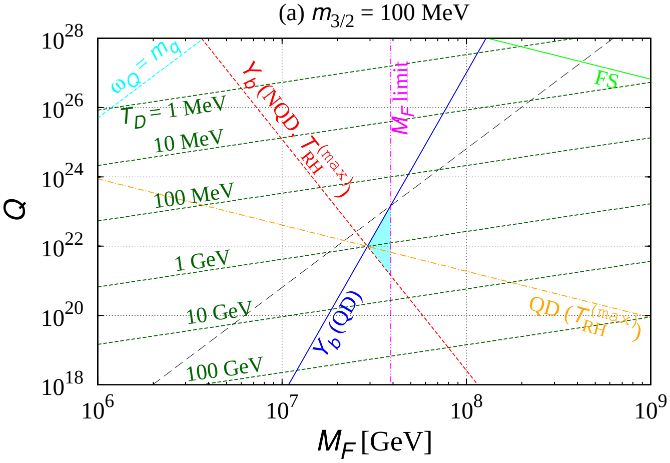

(b) $m_{3/2}$ = 500 MeV

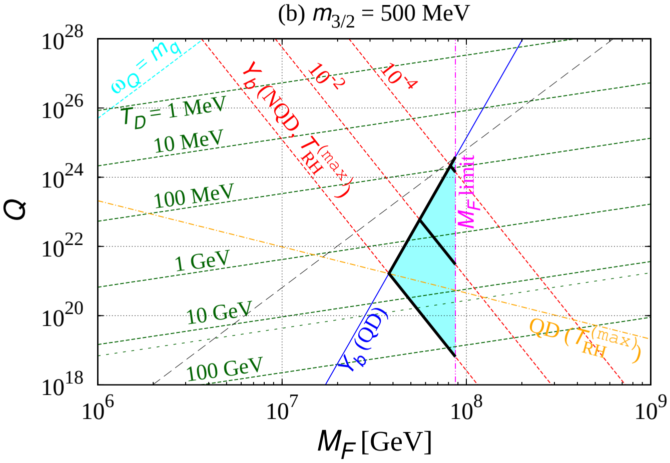

FIG. 2: Allowed region for $m_{3/2}$ = (a) 100 MeV and (b) 500 MeV, which is surrounded by the Y_b line for QD case (blue solid line) and for NQD case with $T_{\rm RH}$ being fixed (red dashed line), and by M_F limit (magenta double-dotted dashed line). Iso-T_D contours are shown in dark green lines. We also show the kinematical limit (cyan dashed) and the free streaming constraint (green solid). Black long dashed line represents the trace of the upper limit of the allowed region when $m_{3/2}$ changes.

Together with the upper limit (3) on M_F, shown in magenta double-dotted dashed lines in Fig. 2, we have the allowed regions in the parameter space (M_F, Q). We show in Fig. 2 two cases with different gravitino masses: (a) 100 MeV and (b) 500 MeV.

The boundary of the Q-ball domination/non-domination is derived from the relation

$$1 = \left.\frac{\rho_Q}{\rho_r}\right|_{\rm D} \simeq \frac{16}{9}\frac{\omega_Q}{T_{\rm D}}(\varepsilon b)^{-1}Y_b \simeq 6.9\times10^{-4}\left(\frac{\zeta}{2.5}\right)^{1/2}\left(\frac{N_q}{18}\right)^{-1/2}\left(\frac{N_{\rm D}}{61.75}\right)^{1/4} \times\left(\frac{T_{\rm RH}}{10^4\ {\rm GeV}}\right)\left(\frac{M_F}{10^7\ {\rm GeV}}\right)^{3/2}\left(\frac{Q}{10^{22}}\right)^{9/8}, \quad (41)$$

where we use Eqs.(25), (19), and the lower equation in Eq.(24). This leads to the following boundary of the Q-

ball dominance on (M_F,Q) parameter space, given by

$$Q \simeq 6.5\times 10^{24}\left(\frac{\zeta}{2.5}\right)^{-4/9}\left(\frac{N_q}{18}\right)^{4/9}\left(\frac{N_{\rm D}}{61.75}\right)^{-2/9} \times\left(\frac{T_{\rm RH}}{10^4\ {\rm GeV}}\right)^{-8/9}\left(\frac{M_F}{10^7\ {\rm GeV}}\right)^{-4/3}, \quad (42)$$

above (below) which corresponds to the (N)QD case, shown in orange dotted-dashed lines in Fig. 2.

As $T_{\rm RH}$ decreases to lower values, the baryon abundance line in NQD case sweeps the hatched region. We show two cases of $T_{\rm RH}/T_{\rm RH}^{\rm (max)} = 10^{-2}$ and 10^{-4} in Fig. 2(b).

The allowed region for $m_{3/2} = 100$ MeV shown in Fig. 2(a) applies to stau and sneutrino NLSPs, while it does not to the bino, as can be seen from Fig. 1 that the decay temperature should be $\gtrsim 10$ GeV for the bino NLSP in order to evade the BBN constraint, while $\gtrsim$ a few MeV is possible for stau and sneutrino NLSP. Similarly, the allowed region for $m_{3/2} = 500$ MeV is applicable to stau and sneutrino cases, while the bino case is allowed only for $T_D \gtrsim 16$ GeV (below the dotted line). (See also Fig. 1(a) where we show $T_D \simeq 16$ GeV in dotted line.)

Black long dashed lines show the trace of the upper bound of allowed regions when $m_{3/2}$ is changed. Therefore, the whole allowed region is below this long dashed line and above red short dashed line, and the lower limit of the gravitino mass is obtained as $m_{3/2} \gtrsim 42$ MeV. On the other hand, one can take larger gravitino mass of O(GeV) in the stau case, and even much larger in the sneutrino case, as can be seen from Fig. 1. It is allowed typically for $T_{\rm D} \gtrsim 10$ GeV, which corresponds to the lower part in (M_F, Q) plane. It will eventually constrained by the fact that such small charge Q balls may evaporate in the thermal bath, or the Q ball cannot be the gauge-mediation type, where the logarithmic term can no longer dominate over the mass term (See Eq.(1)).

Now let us check that the allowed regions obtained above are consistent with more general conditions, which indeed turns out that they are less restrictive. We show the decay temperature T_D in dark green lines, the kinematical bound $\omega_Q > m_q$ in cyan lines, and the free streaming limit in green lines in Fig. 2.

First we see the constraint on the decay temperature $T_{\rm D}$. Since the decay of the Q ball should take place before the BBN, the decay temperature must be larger than ∼MeV. The $T_{\rm D}$ contour is given by

$$Q \simeq 5.3\times 10^{26}\left(\frac{\zeta}{2.5}\right)^{4/5}\left(\frac{N_q}{18}\right)^{4/5}\left(\frac{N_{\rm D}}{10.75}\right)^{-2/5} \times\left(\frac{T_{\rm D}}{\rm MeV}\right)^{-8/5}\left(\frac{M_F}{10^7\ {\rm GeV}}\right)^{4/5}. \quad (43)$$

Next we consider the kinematical bound. The Q ball is kinematically allowed to decay into quarks. This is achieved for $Q < Q_{\rm D}$ (See Eq.(10)):

$$Q < 5.0\times 10^{29}\left(\frac{\zeta}{2.5}\right)^{4}\left(\frac{M_F}{10^7\ {\rm GeV}}\right)^{4}. \quad (44)$$

In addition, since the gravitino mass is relatively small, the produced gravitinos could free-stream to affect large scale structures. In order to avoid such a case, we impose that the free streaming length should not exceed ∼ Mpc [18], which results in the bound on the present day free streaming velocity as $v_0 \lesssim 3.7\times 10^{-7}$. v_0 is estimated as

$$v_0 \simeq \frac{1}{2}\frac{\omega_Q}{m_{3/2}}\frac{T_0}{T_{\rm D}}\left(\frac{N_0}{N_{\rm D}}\right)^{1/3}, \quad (45)$$

where T_0 and N_0 are respectively the temperature and the relativistic degrees of freedom at present. Therefore, the constraint is obtained as

$$Q \lesssim 3.1\times 10^{29}\left(\frac{\zeta}{2.5}\right)^{-4/3}\left(\frac{N_q}{18}\right)^{4/3}\left(\frac{N_{\rm D}}{10.75}\right)^{2/9} \times\left(\frac{m_{3/2}}{100\ {\rm MeV}}\right)^{8/3}\left(\frac{M_F}{10^7\ {\rm GeV}}\right)^{-4/3}. \quad (46)$$

VI. CONCLUSIONS

We have reinvestigated the scenario that the amount of the baryons and the gravitino dark matter is naturally explained by the decay of the Q balls in the gauge-mediated SUSY breaking. Using the more correct decay rates into gravitinos and baryons derived recently in Ref. [11], and also taking into account the Q-ball domination and/or the free streaming condition, we have found that the scenario actually works. Although the branching into gravitinos is smaller than the previous estimate, which leads to the more relative production of NLSPs by the decay of the Q balls, the actual abundance of the NLSP is suppressed by the annihilation effects.

We have found that the scenario works typically for $m_{3/2} = 40$ MeV $-$ 5 GeV, $M_F = 3\times 10^7 - 3\times 10^8$ GeV, and $Q = 10^{18} - 10^{24}$, although there are some differences among the NLSP species. Therefore, it is natural to have this scenario of simultaneous direct creation of the baryon asymmetry and the gravitino dark matter from the Q-ball decay.

Acknowledgments

S.K. would like to thank Particle and Astroparticle Division of Max-Planck-Institut für Kernphysik, Heidelberg for hospitality. The work is supported by Grant-in-Aid for Scientific Research 23740206 (S.K.), 14102004 (M.K.) and 21111006 (M.K.) from the Ministry of Education, Culture, Sports, Science and Technology in Japan, and also by World Premier International Research Center Initiative (WPI Initiative), MEXT, Japan.

Appendix A: Indirect production of the gravitino dark matter via NLPs

We briefly summarize the case of the indirect production of the gravitino dark matter from the Q-ball decay. The Q ball first decays into NLSPs, which eventually decay into the gravitinos that become the dark matter of the universe. In actual scenario, there are two cases. The one is that the NLSPs annihilate to reduce their abundance to the annihilation density (Eqs.(33) – (35)). This is essentially the same case considered in Ref.[10]. The other is the case that the amount of the NLSPs produced by the Q-ball decay is small enough that they do not annihilate to reduce the amount. In either case, the NLSP abundance should coincide with Eq.(36).

In the former case, where the annihilation is effective, it can be readily read off from Fig. 1 for the allowed range of the gravitino mass $m_{3/2}$ (or equivalenlty, the decay temperature of the Q ball, $T_{\rm D}$):

$$\begin{cases} m_{3/2} = 2.8 - 20 \text{ MeV}, \\ (T_{\rm D} = 3.7 - 26 \text{ MeV}) & \text{(bino)} \\ m_{3/2} = 39 - 500 \text{ MeV}, \\ (T_{\rm D} = 1 - 13 \text{ MeV}) & \text{(stau)} \\ m_{3/2} = (3-5)\times 100 \text{ MeV}. \\ (T_{\rm D} = 1.6 - 3.9 \text{ MeV}) & \text{(sneutrino)} \end{cases} \tag{A1}$$

Notice that the lower bound in the bino NLSP is determined by $\Gamma_Q^{(q)} > \Gamma_{\rm NLSP}$, where the NLSP decay rate is estimated as

$$\Gamma_{\rm NLSP} = \frac{m_{\rm NLSP}^5}{48\pi m_{3/2}^2 M_{\rm P}^2}. \tag{A2}$$

As for the baryon abundance, it is determined by Eq.(24) with appropriate value of ε (and $T_{\rm RH}$).

On the other hand, the latter case appears in relatively narrow range of $T_{\rm D}$. The argument is similar to the direct production discussed in Sec. IV and V. Since the gravitino abundance has straightforward relation to the baryon abundance through the number density of the NLSPs as

$$5 \approx \frac{\rho_{3/2}}{\rho_b} = \frac{m_{3/2}}{m_N}\frac{n_{3/2}}{n_b} \simeq \frac{m_{3/2}}{m_N}\frac{Q_{\rm cr}}{Q}\frac{B_{\rm NLSP}}{\varepsilon b}, \tag{A3}$$

the baryon abundance is estimated as, from Eq.(24),

$$\frac{Y_b^{\rm (QD,indir)}}{10^{-10}} \simeq 9.5\times 10^2 \left(\frac{\zeta}{2.5}\right)^{7/2} \left(\frac{N_q}{18}\right)^{-1/2} \times \left(\frac{N_{\rm D}}{10.75}\right)^{-1/4} \left(\frac{m_{\rm NLSP}}{300 \text{ GeV}}\right)^{-4} \left(\frac{m_{3/2}}{20 \text{ MeV}}\right) \times \left(\frac{M_F}{10^7 \text{ GeV}}\right)^{7/2} \left(\frac{Q}{10^{22}}\right)^{-11/8}, \tag{A4}$$

when the Q balls dominate the energy density of the universe, and, for the non Q-ball domination case,

$$\frac{Y_b^{\rm (NQD,indir,s)}}{10^{-10}} \simeq 0.42 \left(\frac{\zeta}{2.5}\right)^4 \left(\frac{N_q}{18}\right)^{-1} \times \left(\frac{m_{\rm NLSP}}{300 \text{ GeV}}\right)^{-4} \left(\frac{m_{3/2}}{20 \text{ MeV}}\right) \times \left(\frac{T_{\rm RH}}{10^4 \text{ GeV}}\right) \left(\frac{M_F}{10^7 \text{ GeV}}\right)^5 \left(\frac{Q}{10^{22}}\right)^{-1/4}, \tag{A5}$$

for $\omega_Q < m_{\rm NLSP} (= 300 \text{ GeV})$, and

$$\frac{Y_b^{\rm (NQD,indir,b)}}{10^{-10}} \simeq 0.23 \left(\frac{N_q}{18}\right)^{-1} \left(\frac{m_{3/2}}{20 \text{ MeV}}\right) \times \left(\frac{T_{\rm RH}}{10^4 \text{ GeV}}\right) \left(\frac{M_F}{10^7 \text{ GeV}}\right) \left(\frac{Q}{10^{22}}\right)^{3/4}, \tag{A6}$$

for $\omega_Q > m_{\rm NLSP}$. We therefore obtain the relation between Q and M_F from these estimates with $Y_b = 10^{-10}$. They are shown as an example of the stau and sneutrino NLSP for $m_{3/2} = 500$ MeV in Fig. 3. Thick solid lines denote the case when the annihilation fixes the NLSP density, while the Q-ball decay determines the NLSP density for the hatched regions.

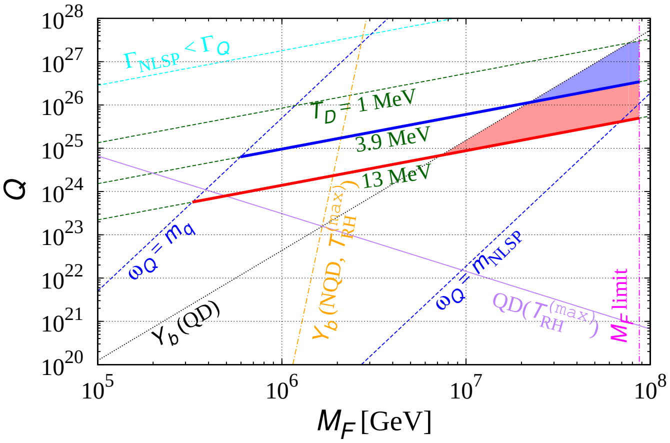

FIG. 3: Allowed region for $m_{3/2} = 200$ MeV. The NLSP (or equivalently the gravitino dark matter) density is fixed by the annihilation (thick solid lines) or determined by the Q-ball decay (hatched regions). Red and blue regions correspond to the stau and sneutrino NLSPs, respectively.

Finally, we comment on the free streaming constraint in the case of the indirect production the gravitino dark matter. Since the decay is determined by the NLSP decay rate (A2), the present-day free streaming velocity is estimated as

$$v_0 \simeq \frac{1}{2}\frac{m_{\rm NLSP}}{m_{3/2}}\frac{T_0}{T_{\rm NLSP}}\left(\frac{N_0}{N_{\rm D}}\right)^{1/3}, \tag{A7}$$

where $T_{\rm NLSP} = \Gamma_{\rm NLPS}^{-1}$. This turns out the constraint on the NLPS mass as $m_{\rm NLSP} \gtrsim 270$ GeV.

[1] S. R. Coleman, Nucl. Phys. B **262**, 263 (1985) [Erratum-ibid. B **269**, 744 (1986)].

[2] A. Kusenko and M. E. Shaposhnikov, Phys. Lett. B **418**, 46 (1998).

[3] K. Enqvist and J. McDonald, Phys. Lett. B **425**, 309 (1998).

[4] S. Kasuya and M. Kawasaki, Phys. Rev. D **61**, 041301(R) (2000).

[5] S. Kasuya and M. Kawasaki, Phys. Rev. D **62**, 023512 (2000).

[6] S. Kasuya and M. Kawasaki, Phys. Rev. D **64**, 123515 (2001).

[7] I. M. Shoemaker and A. Kusenko, Phys. Rev. D **80**, 075021 (2009).

[8] F. Doddato and J. McDonald, JCAP **1106**, 008 (2011); JCAP **1206**, 031 (2012).

[9] S. Kasuya and M. Kawasaki, Phys. Rev. D **84**, 123528 (2011).

[10] F. Doddato and J. McDonald, arXiv:1211.1892 [hep-ph].

[11] M. Kawasaki and M. Yamada, arXiv:1209.5781 [hep-ph].

[12] A. de Gouvêa, T. Moroi and H. Murayama, Phys. Rev. D **56**, 1281 (1997).

[13] J. Hisano, M. M. Nojiri and N. Okada, Phys. Rev. D **64**, 023511 (2001).

[14] A. G. Cohen, S. R. Coleman, H. Georgi and A. Manohar, Nucl. Phys. B **272**, 301 (1986).

[15] J. L. Feng, S. Su and F. Takayama, Phys. Rev. D **70**, 075019 (2004).

[16] M. Kawasaki, K. Kohri, T. Moroi and A. Yotsuyanagi, Phys. Rev. D **78**, 065011 (2008).

[17] M. Kawasaki, F. Takahashi and T. T. Yanagida, Phys. Rev. D **74**, 043519 (2006).

[18] J. Hisano, K. Kohri and M. M. Nojiri, Phys. Lett. B **505**, 169 (2001); F. D. Steffen, JCAP **0609**, 001 (2006).